BULLETIN OF THE POLISH ACADEMY OF SCIENCES
TECHNICAL SCIENCES, Vol. 69(2), 2021, Article number: e136733
DOI: 10.24425/bpasts.2021.136733

POWER SYSTEMS AND POWER ELECTRONICS

Traction power supply with three paralleled single phase voltage source inverters

Tadeusz PŁATEK[1]*, Tomasz OSYPINSKI[2], and Zdziaław CHŁODNICKI[2]

[1] Institute of Control and Industrial Electronics, Warsaw University of Technology, Koszykowa 75, 00-662 Warsaw, Poland
[2] Medcom Company, Jutrzenki 78A, 02-315 Warsaw, Poland

Abstract. Installation and operation of rail vehicles powered by multiple system voltages forces the construction of multi-system traction substation. The article describes a traction substation power supply with 15 kV output voltage and frequency Hz and 25 kV at 50 Hz. The topology of the power electronics system and the control structure of the power supply enables parallel connection of several power supplies. The selected topology and control structure ensures minimizing the rms value of the LCRL filter capacitor current used at the output of the inverters. The article analyses the influence of harmonics consumed by the active front end (AFE) rectifier used in traction vehicles on the rms current of the LCRL filter capacitor.

Key words: asymmetrical regular sampled PWM; voltage source inverters; traction power supply; active front end.

1. Introduction

The ZT600-2UIC power supply unit generates two sinusoidal voltages with values of 25 kV (50 Hz) and 15 kV ($16\frac{2}{3}$ Hz) for the traction cables of rolling stock vehicles. It enables testing of electrical equipment of railway vehicle with the appropriate voltage, supplied to the traction wire. The power supply unit, equipment of traction substation, is a symmetrical load to medium voltage 3×15 kV power grid with a low content of higher harmonics of the consumed current.

The selected topology of the power supply system and control algorithm ensures that the *rms* value of the LCRL output filter capacitor current forced by ripple current output currents of inverter branches is minimized.

Referenced works [1–5] indicate positive impact of using the system with parallel interleaved inverters on minimizing higher harmonics in output currents of LCRL filter. This paper presents the relationship for determining the *rms* value of the capacitor current components C forced by three parallel connected interleaved voltage source inverters (the novelty aspect presented in this document).

The *rms* value of the capacitor current in the LCRL filter is influenced much more by a load on the power supply which is the active front end (AFE) rectifier used in traction vehicles. In the scientific and technical literature there are many studies on the harmonics taken by AFEs installed in rail vehicles [1, 6, 7], but these studies discuss cases where a voltage generator or one phase of a three-phase power supply system with high short-circuit power is the power source. An analysis of a system with an LCRL filter with two AFE systems connected in parallel on the AC side and in parallel on the DC side was conducted in [8]. This work discusses such a system and gives relations allowing to determine the *rms* values of the harmonics taken by this load (the novelty aspect presented in this document).

2. Description of the power supply

The ZT600-2UIC power supply consists of a 12-pulse rectifier (Fig. 1) and three paralleled single phase voltage source inverters (Fig. 2) and a 400 V/15 kV transformer with an additional tap (II) on the low voltage side enabling the generation 25 kV voltage at the transformer output. The output power of the power supply is 600 kW with an overload capacity of 1200 kW for 1 min. The device is powered from the T_{r1} transformer connected to the 3×15 kV power network. The input circuit of the power supply has B1 and B2 fused switch disconnectors. The input voltage is supplied to a 12-pulse rectifier (D1–D12), which supplies the DC link of parallel connected inverters, producing a voltage of 50 Hz or $16\frac{2}{3}$ Hz. The output voltage is fed to the T_{r2} transformer, which generates 25 kV and 15 kV. Figure 1 also shows a typical load of the power supply, i.e., the active front end rectifier, currently commonly used in rail vehicles [5, 6, 8].

Figure 3 shows the power supply unit control system. u_{T1}, u_{T2}, u_{T3} auxiliary waveforms are used in modulators producing control pulses of Q1G-Q6G and Q1D-Q6D transistors in a way resulting from the pattern shown in Fig. 3. Using a system with three interleaved one phase voltage source inverters enables a significant improvement of the quality of the power supply unit output voltage. The control system uses a serial system of voltage and current controllers. To regulate the *rms* value of the $U_{ab,rms}$ output voltage, a PI type regulator with K_{iu} param-

*e-mail: tadeusz.platek@ee.pw.edu.pl

Manuscript submitted 2020-07-30, revised 2020-10-21, initially accepted for publication 2020-11-09, published in April 2021

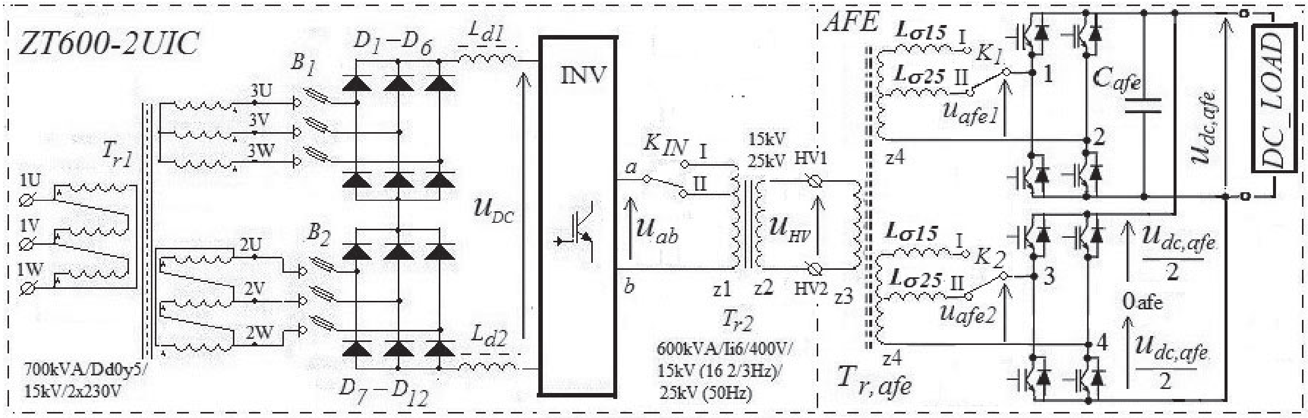

Fig. 1. Block diagram of the power supply unit with active front end rectifier connected to the output terminals

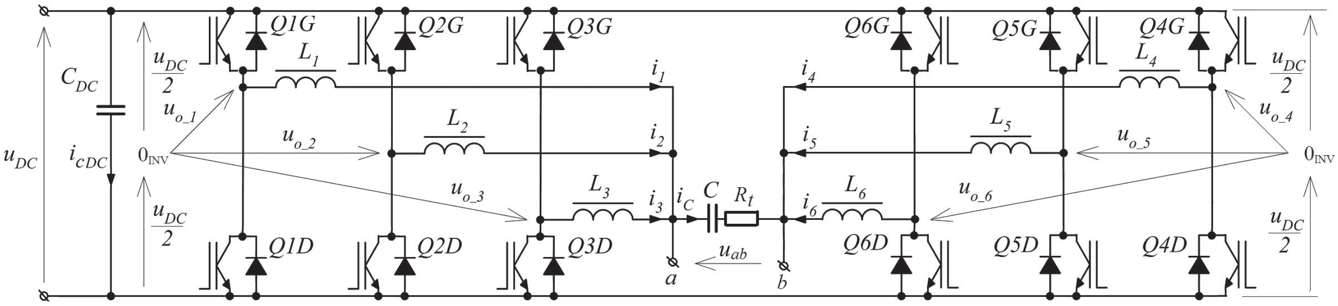

Fig. 2. Diagram of three paralleled one phase voltage source inverters

eters was used. Whereas the uniform distribution of currents i_1, i_2, i_3, i_4, i_5 and i_6, measured with k_i gain transducers, is ensured by proportional controllers with K_r gain. The multiplier system (k_M) allows to create a sinusoidal signal that gives u_i currents.

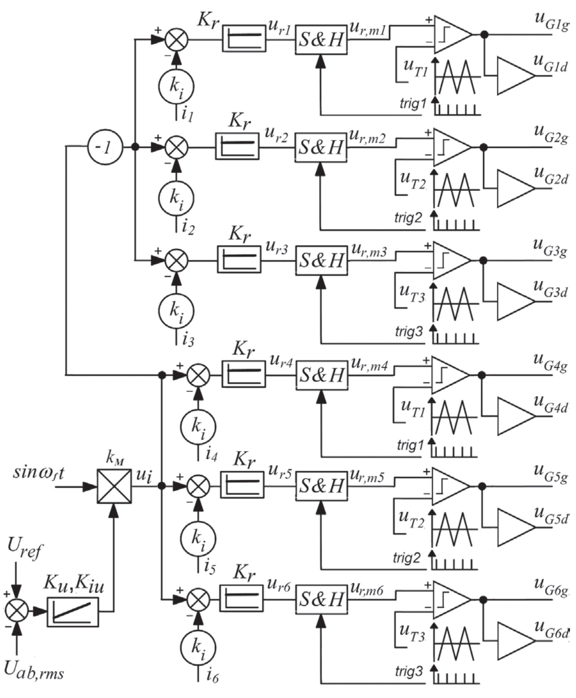

Fig. 3. Power supply unit control system

3. Harmonics output voltage of the half-bridge (one phase leg) voltage source inverter

Figure 4 shows the triangular auxiliary voltages u_{T1}, u_{T2} and u_{T3}, while Fig. 5 shows the voltages in the asymmetrical regular sampled PWM modulator. Sinusoidal output voltage of the current controller is a special case, convenient for analysing modulator properties. The $u_{r,m}$ time waveform is the output voltage of the S&H sample and hold system. The lower part of Fig. 5 shows the relative output voltage of the inverter branch described by the relation:

$$\vec{u}_o = 2\,(u_o/U_{DC}), \tag{1}$$

$$\xi = \omega_c/\omega_f, \tag{2}$$

where ω_c is the pulsation of the triangular carrier, ω_f is the angular frequency of u_r voltage.

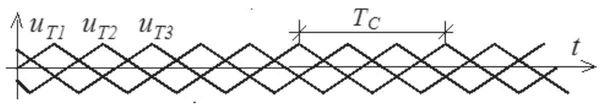

Fig. 4. Triangular modulator carrier signals

As the voltage $\overline{u}_o$ was related to the "0_{INV}" potential (Fig. 2), the value of the constant component is equal to zero. In work [9], there are relations describing output voltage of the tran-

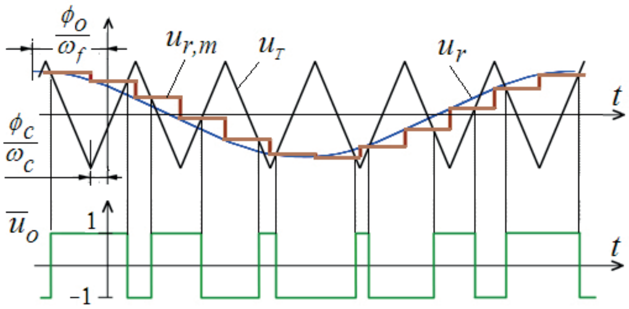

Fig. 5. Signal waveforms in a system with asymmetrical regular sampled PWM modulator

sistor branch $\overline{u}_o$ produced in a double-sampling system (asymmetrical regular sampled PWM). The course of $\overline{u}_o$ is a periodic function with ω_f pulsation if the multiple of ξ pulsations of u_T and u_r is an integer.

$$\vec{u}_o = \sum_{n=1}^{\infty} F_{0n} \cos\left(n\left[\omega_f t + \phi_o\right]\right) + \sum_{\rho=1}^{\infty} \sum_{n=-\infty}^{\infty} F_{\rho n} \cos\left(\rho\left[\omega_c t + \phi_c\right] + n\left[\omega_f t + \phi_o\right]\right) \tag{3}$$

with ϕ_o, ϕ_c being the initial phases of low-frequency input wave u_r and auxiliary triangular voltage u_T respectively. F_{0n}, $F_{\rho n}$ are harmonic coefficients. Relation (3) can be presented in a different form, allowing direct reading of the order and initial phase of each harmonic for the i-th branch of the inverter:

$$\vec{u}_{o\_i} = \sum_{n=1}^{\infty} F_{0n} \cos\left(n\omega t + n\phi_{oi}\right) + \sum_{\rho=1}^{\infty} \sum_{n=-\infty}^{\infty} F_{\rho n} \cos\left(\left[\rho\xi + n\right]\omega_f t + \rho\phi_{ci} + n\phi_{oi}\right), \tag{4}$$

where $i = 1, 2, 3, 4, 5, 6$.

The phases ϕ_o and ϕ_c for each branch assume values:
$\phi_{o1} = \phi_{o2} = \phi_{o3} = 0$, $\phi_{o4} = \phi_{o5} = \phi_{o6} = \pi$,
$\phi_{c1} = \phi_{c4} = 0$, $\phi_{c2} = \phi_{c5} = -2\pi/3$, $\phi_{c3} = \phi_{c6} = 2\pi/3$.

Fundamental and baseband harmonics coefficient ($k = n = 1, 2, 3 \ldots \infty$, $\rho = 0$) are described by the following relations:

$$F_k = F_{0n} = \frac{4\xi}{n\pi} J_n\left(n\frac{\pi M}{2\xi}\right) \sin n\frac{\pi}{2}, \tag{5}$$

where $J_k(x)$ denotes a Bessel function of the first type, M indicates the modulation depth factor:

$$M = \hat{U}_r / U_T, \tag{6}$$

where $\hat{U}_r$ is the amplitude of the low frequency u_r control waveform, U_T is the maximum value of the auxiliary triangular waveform.

For $\xi \geq 10$ the following approximation [3] (with an error not exceeding 0.3%) is true:

$$\frac{4\xi}{\pi} J_1\left(\frac{\pi M}{2\xi}\right) \approx M \tag{7}$$

so, we can use an approximation:

$$F_{01} = M. \tag{8}$$

The initial phases Ψ_{ki} of the harmonic output voltages of the individual branches for the above harmonic group are determined from the following relation:

$$\psi_{ki} = n\phi_{oi}. \tag{9}$$

Coefficients and initial phases Ψ_{ki} for carrier harmonics ($k = \rho\xi + n, n = 0, \rho = 1, 2, \ldots, \infty$) and sideband harmonics ($n = -\infty \ldots, -2, -1, 1, 2 \ldots \infty$, $\rho = 1, 2, \ldots, \infty$) are describe by:

$$F_k = F_{\rho n} = \frac{4}{\pi} \frac{J_n\left(\left[\rho + {}^{n}\!/_{\xi}\right]\frac{\pi M}{2}\right)}{\rho + {}^{n}\!/_{\xi}} \sin\left(\left[\rho + n\right]\frac{\pi}{2}\right), \tag{10}$$

$$\psi_{ki} = \rho\phi_{ci} + n\phi_{oi}. \tag{11}$$

$F_{\rho n}$ and $F_{\rho\xi+n}$ labels are the same ($F_{\rho n} = F_{\rho\xi+n}$).

4. Harmonics of the algebraic sum of the output voltages of the inverter branches

After substituting appropriate value of the phase ϕ_c in (4) (0 for Q1, $-2\pi/3$ for Q2 and $2\pi/3$ for Q3) and $\phi_o = 0$ for each branch we obtain a relation describing the sum of relative output voltages of three branches (Q1, Q2, Q3) related to $U_{DC}/2$.

$$\vec{u}_{o\_1} + \vec{u}_{o\_2} + \vec{u}_{o\_3} = 3\sum_{n=1}^{\infty} F_{0n} \cos\left(n\omega_f t\right) + \sum_{\rho=1}^{\infty} \sum_{n=-\infty}^{\infty} F_{\rho n} \cos\left(\left[\rho\xi + n\right]\omega_f t\right)\left\{1 + 2\cos\rho\frac{2}{3}\pi\right\}. \tag{12}$$

After substituting to (4) the appropriate value of the phase ϕ_c (0 for Q4, $-2\pi/3$ for Q5 and $2\pi/3$ for Q6) and $\phi_o = \pi$ for each branch we obtain a relation describing the sum of relative output voltages of the three branches (Q4,Q5,Q6) related to U_{DC}/2.

$$\vec{u}_{o\_4} + \vec{u}_{o\_5} + \vec{u}_{o\_6} = 3\sum_{n=1}^{\infty} F_{0n} \cos\left(n\left[\omega_f t + \pi\right]\right) + \sum_{\rho=1}^{\infty} \sum_{n=-\infty}^{\infty} F_{\rho n} \cos\left(\left[\rho\xi + n\right]\omega_f t\right) \cos n\pi \left\{1 + 2\cos\rho\frac{2}{3}\pi\right\}. \tag{13}$$

Let us mark by $\bar{u}_\Sigma$ algebraic sum of output voltages of all three inverter branches:

$$\sum_{i=1}^{3} \vec{u}_{o\_i} - \sum_{i=4}^{6} \vec{u}_{o\_i} = \vec{u}_\Sigma. \tag{14}$$

The $\bar{u}_{\Sigma}$ voltage is determined by subtracting Eqs. (12) and (13):

$$\vec{u}_{\Sigma} = 3\sum_{n=1}^{\infty} F_{0n}\left(1-\cos n\pi\right)\cos\left(n\omega_f t\right) + \sum_{\rho=1}^{\infty}\sum_{n=-\infty}^{\infty} F_{\rho n} N(n,\rho)\cos\left(\left[\rho\xi+n\right]\omega_f t\right), \tag{15}$$

where $N(n,\rho)$ defines the relation:

$$N(n,\rho) = \{1-\cos(n\pi)\}\left\{1+2\cos\rho\frac{2}{3}\pi\right\}. \tag{16}$$

In relations (15) and (16) describing the $\bar{u}_{\Sigma}$ there is no carrier harmonics of the order of $\rho\xi$ because for $n=0$ the coefficient $N(n,\rho)$ =0.

Sideband harmonics coefficient of the oder $k=\rho\xi+n$ determined for $\bar{u}_{\Sigma}$ describes the relation:

$$F_{\rho n}^{(\Sigma)} = \frac{4}{\pi}\frac{J_n\left(\left[\rho+{}^{n}/_{\xi}\right]\frac{\pi M}{2}\right)}{\rho+{}^{n}/_{\xi}}\sin\left(\left[\rho+n\right]\frac{\pi}{2}\right)N(n,\rho). \tag{17}$$

Sideband harmonics coefficient $F_{\rho\xi+n}^{(\Sigma)}$ takes zero values if n is even or $\rho = 1,2,4,5,7,8,10\ldots$ because if any of these conditions is true $N(n,p) = 0$. From the formulae (15) and (16) it follows that the algebraic sum of voltages u_{Σ} contains only harmonics being a multiple of the basic harmonic order $k=n$ if n takes odd values and of the order $k=\rho\xi+n$ if ρ takes a value equal to a multiple of 3 while n is odd. Relation (17) yields zero value of the coefficient $F_{\rho\xi+n}^{(\Sigma)}$ if the sum of $\rho+n$ takes an even value. From these conditions it follows that harmonics of the order $k=\rho\xi+n$ occur for ρ being a multiple of 6 and for n assuming odd values.

4.1. Harmonic output currents of inverter branches with a three phase positive and negative sequence. The harmonic spectra of i_1, i_2, i_3, i_4, i_5 and i_6 currents (Fig. 10a shows the amplitude of the $\hat{I}_{1,k}$) contain fundamental harmonics, harmonics of the order $k=\rho\xi+n$ for ρ being a multiple of 6 and an odd sum of $\rho+n$ and harmonics flowing only in the circuits shown in Fig. 6. The first two harmonic groups form three-phase zero sequences and flow through the C capacitor.

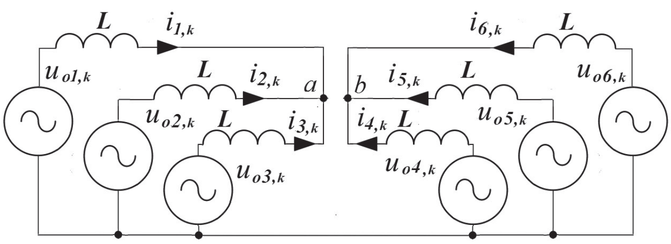

Fig. 6. Equivalent scheme for harmonic output currents of positive and negative sequences of inverter branches

If the k-th harmonics of the voltages $u_{o\_1,k}$, $u_{o\_2,k}$, $u_{o\_3,k}$ form three-phase positive or negative sequences then the sum of $i_{1,k}+i_{2,k}+i_{3,k}$ harmonic currents is zero. Similarly for k-th $u_{o\_4,k}$, $u_{o\_5,k}$, $u_{o\_6,k}$ harmonic voltages with a three-phase positive or negative sequence then the sum of $i_{4,k}+i_{5,k}+i_{6,k}$ harmonic currents equal to zero.

The analysis of the form of relations (10) and (15) shows that in the circuits shown in Fig. 6 harmonics of currents flow for $k=\rho\xi+n$ if $\rho = 1,2,4,5,7,8\ldots$ and $\rho+n$ takes odd values. The harmonics of currents of these orders do not flow in the C capacitor.

5. Harmonics of AC voltage of AFE converters

Figure 1 shows a schematic diagram of a traction power supply unit loaded by means of a multi-winding transformer $T_{r,afe}$ and two AFE bridge circuits connected to each other on the terminal side of DC circuits of $u_{dc,afe}$ voltage. The time courses of u_{afe1} and u_{afe2} voltages are produced in a circuit with an asymmetrical regular sampled PWM modulator (ARS). Relative output voltages of converter branches are described by relations:

$$\vec{u}_{10afe} = 2\left(u_{10afe}/U_{DC,afe}\right), \tag{18}$$

$$\vec{u}_{20afe} = 2\left(u_{20afe}/U_{DC,afe}\right). \tag{19}$$

A $\bar{u}_{10afe}$ waveform is a periodic function with ω_f pulsation if ξ_{afe} (quotient of the u_{T_afe} and u_{r_afe} pulsations) given by the relation:

$$\xi_{afe} = \omega_c^{(afe)}/\omega_f \tag{20}$$

is an integer. $\omega_c^{(afe)}$ is the pulsation of the triangular carrier of the AFE modulator.

Each bridge of the system produces a unipolar voltage output waveform (u_{afe1} or u_{afe2}) by providing the following initial phases of modulating waveforms:

$$\phi_o^{(10afe)} = \phi_o^{(30afe)} = \phi_o^{(afe)}, \tag{21}$$

$$\phi_o^{(20afe)} = \phi_o^{(40afe)} = \phi_o^{(afe)} - \pi. \tag{22}$$

This control provides a twofold increase in the minimum dominant pulsation of the higher output harmonics of u_{afe1} and u_{afe2}, while another twofold increase in the dominant pulsation of the higher output harmonic of u_{afe} voltage is provided by a phase shift in the auxiliary waveforms in modulators used in both bridge systems:

$$\phi_c^{(10afe)} = \phi_c^{(20afe)} = \phi_c^{(afe)}, \tag{23}$$

$$\phi_c^{(30afe)} = \phi_c^{(40afe)} = \phi_c^{(afe)} \pm \frac{\pi}{2}. \tag{24}$$

According to [9], the $\bar{u}_{10afe}$ voltage can be written as:

$$\vec{u}_{10afe} = \sum_{n=1}^{\infty} F_{0n}^{(afe)}\cos n\left[\omega_f t + \phi_o^{(afe)}\right] + \sum_{\rho=1}^{\infty}\sum_{n=-\infty}^{\infty} F_{\rho n}^{(afe)}\cos\left(\begin{matrix}\rho\left[\omega_c^{(afe)} t + \phi_c^{(afe)}\right]\\ +n\left[\omega_f t + \phi_o^{(afe)}\right]\end{matrix}\right). \tag{25}$$

The fundamental and baseband harmonics coefficient ($k = n = 1,2,3\ldots,\infty$) are described by relations (5) while the carrier and sideband harmonics coefficient are described by the relation (10). The parameters of relations (5), (10) are M_{afe} and ξ_{afe}. This can be shown in equation: $F_{\rho n}^{(afe)} = F_{\xi afe+n}(M_{afe})$.

Formula (10) shows that the coefficients $F_{\rho n}^{(afe)}$ take non-zero values if the sum of $\rho + n$ is an odd number.

The voltage $\bar{u}_{20afe}$ describes a relation of a similar form as (25) taking into account another value of the initial phase $\phi_o^{(20afe)}$ of the modulating voltage:

$$\vec{u}_{20afe} = \sum_{n=1}^{\infty} F_{0n}^{(afe)} \cos n\left[\omega_f t + \phi_o^{(afe)} - \pi\right] + \sum_{\rho=1}^{\infty}\sum_{n=-\infty}^{\infty} F_{\rho n}^{(afe)} \cos\left(\begin{array}{l}\rho\left[\omega_c^{(afe)} t + \phi_c^{(afe)}\right]\\ +n\left[\omega_f t + \phi_o^{(afe)} - \pi\right]\end{array}\right). \tag{26}$$

The relative output AC voltage of the H-bridge converter $\bar{u}_{afe1}$ can be determined as the difference between $\bar{u}_{10afe}$ and $\bar{u}_{20afe}$ and after applying trigonometric identity $\cos\alpha - \cos\beta = -2\sin\dfrac{\alpha+\beta}{2}\sin\dfrac{\alpha-\beta}{2}$ they can be presented in the following form:

$$\vec{u}_{afe1} = -2\sum_{n=1}^{\infty} F_{0n}^{(afe)} \sin\frac{n\pi}{2} \sin n\left[\omega_f t + \phi_o^{(afe)} - \frac{\pi}{2}\right] - 2\sum_{\rho=1}^{\infty}\sum_{n=-\infty}^{\infty} F_{\rho n}^{(afe)} \sin\frac{n\pi}{2} \sin\left(\begin{array}{l}\rho\left[\omega_c^{(afe)} t + \phi_c^{(afe)}\right]\\ +n\left[\omega_f t + \phi_o^{(afe)} - \frac{\pi}{2}\right]\end{array}\right). \tag{27}$$

For $n = 2,4,6\ldots$ the harmonics described by the first component disappear and for $n = \pm 0,2,4,6\ldots$ the phrases of the second component disappear. The second property means that all harmonics concentrated at carrier harmonics of $k = \rho\xi_{afe} \pm 0,2,4,6\ldots$ in the spectrum do not exist. This is due to the fact that coefficients $F_{\rho n}^{(afe)}$ take non-zero values if the sum of $\rho + n$ is an odd number, which in turn leads to the next conclusion that the harmonics for which $n = \pm 0,2,4,6\ldots$ are concentrated near the carrier harmonics for $\rho = 1,3,5\ldots$

Voltage $\bar{u}_{afe2} = \bar{u}_{30afe} - \bar{u}_{40afe}$ can be presented in a similar form as (27) including (24):

$$\begin{aligned}\vec{u}_{afe2} = &-2\sum_{n=1}^{\infty} F_{0n}^{(afe)} \sin\frac{n\pi}{2} \sin n\left[\omega_f t + \phi_o^{(afe)} - \frac{\pi}{2}\right]\\ &-2\sum_{\rho=1}^{\infty}\sum_{n=-\infty}^{\infty} F_{\rho n}^{(afe)} \sin\frac{n\pi}{2}\\ &\cdot\sin\left(\begin{array}{l}\rho\left[\omega_c^{(afe)} t + \phi_c^{(afe)} \pm \frac{\pi}{2}\right]\\ +n\left[\omega_f t + \phi_o^{(afe)} - \frac{\pi}{2}\right]\end{array}\right).\end{aligned} \tag{28}$$

The algebraic sum of the voltage of $\bar{u}_{afe1}$ and $\bar{u}_{afe2}$ may be represented by the trigonometric identity $\sin(\alpha - \pi/2) = \sin\alpha\cos(n\pi/2) - \cos\alpha\sin(n\pi/2)$ in form:

$$\begin{aligned}\vec{u}_{afe1} + \vec{u}_{afe2} = &-4\sum_{n=1}^{\infty} F_{0n}^{(afe)} \sin\frac{n\pi}{2} \sin n\left[\omega_f t + \phi_o^{(afe)} - \frac{\pi}{2}\right]\\ &-\sum_{\rho=1}^{\infty}\sum_{n=-\infty}^{\infty} F_{\rho n}^{(afe)}\left\{\begin{array}{l}\sin n\pi \sin\left(\begin{array}{l}\rho\left[\omega_c^{(afe)} t + \phi_c^{(afe)}\right]\\ +n\left[\omega_f t + \phi_o^{(afe)}\right]\end{array}\right)\\ -2\sin^2\frac{n\pi}{2}\cos\left(\begin{array}{l}\rho\left[\omega_c^{(afe)} t + \phi_c^{(afe)}\right]\\ +n\left[\omega_f t + \phi_o^{(afe)}\right]\end{array}\right)\\ +\sin n\pi \sin\left(\begin{array}{l}\rho\left[\omega_c^{(afe)} t + \phi_c^{(afe)} \pm \frac{\pi}{2}\right]\\ +n\left[\omega_f t + \phi_o^{(afe)}\right]\end{array}\right)\\ -2\sin^2\frac{n\pi}{2}\cos\left(\begin{array}{l}\rho\left[\omega_c^{(afe)} t + \phi_c^{(afe)} \pm \frac{\pi}{2}\right]\\ +n\left[\omega_f t + \phi_o^{(afe)}\right]\end{array}\right)\end{array}\right\}.\end{aligned} \tag{29}$$

Since for even values of n disappear the words of the first and second component, for odd values of n the equations $\sin(n\pi) = 0$ and $\sin^2(n\pi/2) = 1$ are met, then (29) can be simplified to the form valid for $n = \pm 1, \pm 3, \pm 5$.

$$\begin{aligned}\vec{u}_{afe1} + \vec{u}_{afe2} = &-4\sum_{n=1}^{\infty} F_{0n}^{(afe)} \sin\frac{n\pi}{2} \sin n\left[\omega_f t + \phi_o^{(afe)} - \frac{\pi}{2}\right]\\ &+2\sum_{\rho=1}^{\infty}\sum_{n=-\infty}^{\infty} F_{\rho n}^{(afe)}\left\{\begin{array}{l}\left[1+\cos\rho\frac{\pi}{2}\right]\cos\left(\begin{array}{l}\rho\left[\omega_c^{(afe)} t + \phi_c^{(afe)}\right]\\ +n\left[\omega_f t + \phi_o^{(afe)}\right]\end{array}\right)\\ -\sin\rho\frac{\pi}{2}\sin\left(\begin{array}{l}\rho\left[\omega_c^{(afe)} t + \phi_c^{(afe)}\right]\\ +n\left[\omega_f t + \phi_o^{(afe)}\right]\end{array}\right)\end{array}\right\}.\end{aligned} \tag{30}$$

Because $F_{\rho n}^{(afe)}$ takes a non-zero value only if the sum of $\rho + n$ has an odd value – this is shown in formula (10) – and the second component for even values of n has a zero value, the second component may be non-zero only for even values of ρ. The formulae above results in that for $\rho = 2.6, 10\ldots$ the second component has a zero value. Thus, for $\rho = 0, \pm, 4, \pm 8\ldots$ applies:

$$\vec{u}_{afe1} + \vec{u}_{afe2} = -4\sum_{n=1}^{\infty} F_{0n}^{(afe)} \sin\frac{n\pi}{2} \sin n\left[\omega_f t + \phi_o^{(afe)} - \frac{\pi}{2}\right] + 4\sum_{\rho=1}^{\infty}\sum_{n=-\infty}^{\infty} F_{\rho n}^{(afe)} \cos\left(\begin{array}{l}\rho\left[\omega_c^{(afe)} t + \phi_c^{(afe)}\right]\\ +n\left[\omega_f t + \phi_o^{(afe)}\right]\end{array}\right). \tag{31}$$

6. LCRL filter capacitor current harmonics

The replacement diagram of an inverter with two rectifier AFE circuits is shown in Fig. 7. A common designation has been adopted for all inductances of the inverter output branches

$L = L_i$ (for $i = 1\ldots6$) and the input inductances of AFE rectifir L'_σ related to the output circuit of power supply inverters. The circuit with the equivalent input inductance $2L/3$ and output inductance L'_σ, capacitor C and damping resistor R_t forms a filter with LCRL type damping [10–13]. The inductance L'_σ is equal to $L'_{\sigma15}$ and $L'_{\sigma25}$ for the 15 kV and 25 kV systems, respectively.

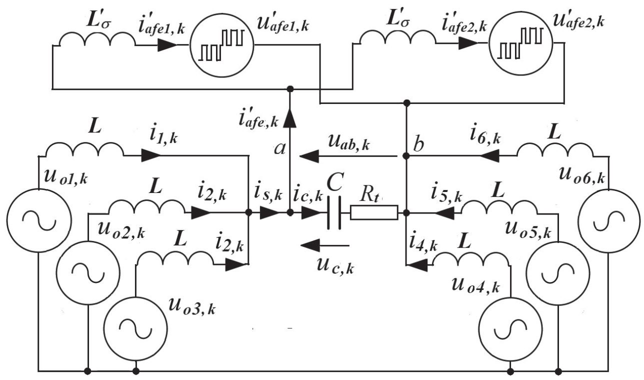

Fig. 7. Replacement diagram for inverter loaded with two *AFE* systems for voltage and current harmonics

Each harmonic can be expressed by complex value. For fundamental and baseband harmonics of the output voltage of the $\bar{u}_{o\_i}$ power supply inverter branch complex voltages are described by the relations:

$$\underline{U}_{oi,n} = U_{o,n} e^{jn\phi_{oi}}, \tag{32}$$

where $U_{o,n}$ is the *rms* value and "i" is the number of inverter branches ($i = 1,2,3,4,5,6$).

Complex value of carrier and sideband harmonics of $\bar{u}_{o\_i}$ voltage takes the form:

$$\underline{U}_{oi,\rho\xi+n} = U_{o,\rho\xi+n} e^{j(\rho\phi_{ci}+n\phi_{oi})}. \tag{33}$$

Complex value of fundamental and baseband harmonics of AFE converter $\bar{u}_{afe1}$ and $\bar{u}_{afe2}$ AC voltages is:

$$\underline{U}_{afe1,n} = \underline{U}_{afe2,n} = U_{afe,n} e^{jn\left(\phi_o^{(afe)}-\frac{\pi}{2}\right)}. \tag{34}$$

Complex value of carrier and sideband harmonics of AFE converter $\bar{u}_{afe1}$ and $\bar{u}_{afe1}$ AC voltages is:

$$\underline{U}_{afe1,\rho\xi+n} = U_{afe,\rho\xi+n} e^{j\left(\rho\phi_c^{(afe)}+n\phi_o^{(afe)}-n\frac{\pi}{2}\right)}, \tag{35}$$

$$\underline{U}_{afe2,\rho\xi+n} = U_{afe,\rho\xi+n} e^{j\left(\rho\left[\phi_c^{(afe)}\pm\frac{\pi}{2}\right]+n\phi_o^{(afe)}-n\frac{\pi}{2}\right)}. \tag{36}$$

Norton law can be used to determine the $\underline{I}_{c,k}$ current. The current flowing between the shorted terminals *ab* has two components:

$$\underline{I}_{ab,k} = \underline{I}_{ab(INV),k} + \underline{I}_{ab(AFE),k} \tag{37a}$$

and it can be determined from the following formula:

$$\underline{I}_{ab,k} = \frac{1}{j2\omega_k L}\left(\sum_{i=1}^{3}\underline{U}_{oi,k} - \sum_{i=4}^{6}\underline{U}_{oi,k}\right) - \frac{1}{j\omega_k L'_\sigma}\left(\underline{U}'_{afe1,k} + \underline{U}'_{afe2,k}\right), \tag{37b}$$

where: $\omega_k = k\omega_f = k2\pi f_f$, $\underline{U}'_{afe1,k}$, $\underline{U}'_{afe2,k}$ are complex voltages referred to the "a–b" output of the power supply unit.

The impedance seen from "a–b" terminals when the voltage sources are shorted is described by the following relation:

$$\underline{Z}_{ab,k} = \frac{j\omega_k - \omega_k^2 CR_t 2LL'_\sigma}{j\omega_k CR_t\left(4L+3L'_\sigma\right) + 4L + 3L'_\sigma - 2\omega_k^2 CLL'_\sigma}. \tag{38}$$

$\underline{U}_{ab,k}$ is equal to $\underline{Z}_{ab,k}\,\underline{I}_{ab,k}$ and is described by formula:

$$\underline{U}_{ab,k} = \frac{\underline{Z}_{ab,k}}{j2\omega_k L}\left(\sum_{i=1}^{3}\underline{U}_{oi,k} - \sum_{i=4}^{6}\underline{U}_{oi,k}\right) - \frac{\underline{Z}_{ab,k}}{j\omega_k L'_\sigma}\left(\underline{U}'_{afe1,k} + \underline{U}'_{afe2,k}\right). \tag{39}$$

Capacitor current $\underline{I}_{c,k}$ is determined from relation:

$$\underline{I}_{c,k} = \frac{j\omega_k C\underline{U}_{ab,k}}{1 + j\omega_k CR_t}. \tag{40}$$

After taking into account in (40) relation (39) we get:

$$\underline{I}_{c,k} = \frac{\underline{Z}_{ab,k}C}{2L\left(1+j\omega_k R_t C\right)}\left(\sum_{i=1}^{3}\underline{U}_{oi,k} - \sum_{i=4}^{6}\underline{U}_{oi,k}\right) - \frac{\underline{Z}_{ab,k}C}{L'_\sigma\left(1+j\omega_k R_t C\right)}\left(\underline{U}'_{afe1,k} + \underline{U}'_{afe2,k}\right). \tag{41}$$

6.1. LCRL filter capacitor current harmonics forced by distorted output current of the power supply inverters. Using the superposition method, we can determine the *rms* values of C capacitor harmonics forced by the distorted output current of the power supply inverter taking into account only the first component of the right-hand side equation (41):

$$\underline{I}_{c(INV),k} = \frac{\underline{Z}_{ab,k}C}{2L\sqrt{1+\left(\omega_k R_t C\right)^2}}\left(\sum_{i=1}^{3}\underline{U}_{oi,k} - \sum_{i=4}^{6}\underline{U}_{oi,k}\right). \tag{42}$$

The amplitude of the algebraic sum of harmonics of the same order of instantaneous voltages is equal to the amplitude of the sum of complex voltages that represent these instantaneous values.

According to the considerations in the previous chapter, there are only harmonics that are a multiple of the basic harmonic order $k = n$ ($\rho = 0$) if n takes odd values and of the order $k = \rho\xi + n$ if ρ takes a value equal to a multiple of 6 while n is odd.

For $k = n$ taking odd values and $\rho = 0$ current amplitude value $\hat{I}_{c(INV),k}$ can be calculated from the following formula:

$$\widehat{I}_{c(INV),k} = \frac{3Z_{ab,n}C}{L\sqrt{1+(\omega_n R_t C)^2}} \frac{U_{DC}}{2} \hat{F}_{0n}\,, \tag{43}$$

where $\hat{F}_{0n} = |F_{0n}|$, F_{0n} describes (5) and $Z_{ab,n}$ gives the formula:

$$Z_{ab,k} = \frac{2\omega_k L L'_\sigma \sqrt{1+(\omega_k C R_t)^2}}{\sqrt{(4L+3L'_\sigma)^2(\omega_k C R_t)^2 + (4L+3L'_\sigma - 2\omega_k^2 CLL'_\sigma)^2}} \tag{44}$$

for $k = n$.

After substituting $n = 1$ to (43) and the relation (44) describing $Z_{ab,1}$ and making several transformations and applying approximation $F_{01} \approx M$ we get:

$$\widehat{I}_{c(INV),1} = \frac{3}{2}\frac{C}{L} \frac{\omega_f L_z U_{DC} M}{\sqrt{(\omega_f C R_t)^2 + \left(1-\omega_f^2/\omega_{res}^2\right)^2}}\,, \tag{45}$$

where:

$$L_z = \frac{2LL'_\sigma}{(4L+3L'_\sigma)}\,, \tag{46}$$

$$\omega_{res} = 1/\sqrt{L_z C}\,. \tag{47}$$

Because $10\omega_f < \omega_{res}$ [14] and $(\omega_f C R_t)^2 \ll 1$, relation (45) can be simplified to:

$$\widehat{I}_{c(INV),1} = \frac{3}{2}\frac{L_z}{L}\omega_f C U_{DC} M\,. \tag{48}$$

For ρ taking the value 6 and its multiples and for n taking the values of odd harmonic current of the capacitor of the order $k = 6\xi + n$ can be determined from the relation:

$$\widehat{I}_{c(INV),6\xi+n} = \frac{3}{2} \frac{Z_{ab,6\xi+n}C}{L\sqrt{1+(\omega_k R_t C)^2}} U_{DC}\hat{F}_{6\xi+n}\,, \tag{49}$$

where $\hat{F}_{6\xi+n} = |F_{6\xi+n}|$, $F_{\rho\xi+n} = F_{\rho n}$ is described by (10).

For $\xi \geq 10$ and $|n| \leq 9$ the following approximation can be used with great accuracy: $Z_{ab,6\xi} \approx Z_{ab,6\xi-n} \approx Z_{ab,6\xi+n}$. After substituting for (49) the relation (44) describing $Z_{ab,6\xi}$ and making several transformations, we obtain:

$$\widehat{I}_{c(INV),\rho\xi+n} = \frac{3}{2}\frac{\omega_{6\xi}}{\omega_{res}^2} \frac{U_{DC}\hat{F}_{6\xi+n}}{L\sqrt{(\omega_{6\xi} C R_t)^2 + \left(1-\omega_{6\xi}^2/\omega_{res}^2\right)^2}}\,, \tag{50}$$

where $\omega_{6\xi} = 6\xi\omega_f$.

After taking into account the inequalities $\omega_{res} \ll \omega_{6\xi}$ [3, 15] and $\omega_{6\xi} C R_t \ll \omega_{6\xi}^2/\omega_{\mathrm{res}}^2$, (50) can be simplified to form:

$$\widehat{I}_{c(INV),\rho\xi+n} \approx \frac{3}{2}\frac{U_{DC}}{\omega_{6\xi}L}\hat{F}_{6\xi+n}\,. \tag{51}$$

Table 1 contains examples of values (for $M = 0, 0.6, 0.9$) of amplitudes $\hat{F}_{6\xi+n}$ for the arguments $(6 \pm n/\xi)\pi M/2$ and values of simplified expressions $\hat{F}^{(*)}_{6\xi+n}$ for $n = 1, 2, \ldots 9$ and $3\pi M$ arguments. On the basis of the results contained in the table and the results for other M values not shown in this table, an approximate relation can be formulated:

$$0.5\left(\hat{F}^2_{6\xi-n} + \hat{F}^2_{6\xi+n}\right) \approx \left(\hat{F}^{(*)}_{6\xi+n}\right)^2, \tag{52}$$

where $\hat{F}_{6\xi+n}$ is the absolute value of the coefficient given by formula (10).

Table 1
Examples of absolute values $\hat{F}_{6\xi+n}$ and $\hat{F}^{(*)}_{6\xi+n}$

$M = 0.2$	$\hat{F}_{6\xi+n}$	$n=-1$	$n=-3$	$n=-5$	$n=-7$	$n=-9$
		0.124	0.023	0.001	0.000	0.000
		$n=1$	$n=3$	$n=5$	$n=7$	$n=9$
		0.123	0.024	0.001	0.000	0.000
	$\hat{F}^{(*)}_{6\xi+n}$	$n=1$	$n=3$	$n=5$	$n=7$	$n=9$
		0.123	0.024	0.001	0.000	0.000
$M = 0.6$	$\hat{F}_{6\xi+n}$	$n=-1$	$n=-3$	$n=-5$	$n=-7$	$n=-9$
		0.071	0.050	0.070	0.019	0.002
		$n=1$	$n=3$	$n=5$	$n=7$	$n=9$
		0.069	0.041	0.072	0.023	0.004
	$\hat{F}^{(*)}_{6\xi+n}$	$n=1$	$n=3$	$n=5$	$n=7$	$n=9$
		0.070	0.046	0.071	0.021	0.003
$M = 0.9$	$\hat{F}_{6\xi+n}$	$n=-1$	$n=-3$	$n=-5$	$n=-7$	$n=-9$
		0.058	0.059	0.025	0.072	0.031
		$n=1$	$n=3$	$n=5$	$n=7$	$n=9$
		0.058	0.053	0.006	0.069	0.040
	$\hat{F}^{(*)}_{6\xi+n}$	$n=1$	$n=3$	$n=5$	$n=7$	$n=9$
		0.058	0.056	0.015	0.072	0.036

The application of (52) introduces an error not exceeding a few %. Simplified relation $\hat{F}^{(*)}_{\rho\xi+n} = \hat{F}_{\rho\xi+n}$ for $n/\xi \ll \rho$ is in form:

$$\hat{F}^{(*)}_{\rho n} = \hat{F}^{(*)}_{\rho\xi+n} = \frac{4}{\rho\pi}\left|J_n(\rho\pi M/2)\right|. \tag{53}$$

The resulting *rms* value of harmonics of the order close to 6ξ can be determined from the following formula:

$$I_{c,6\xi} \approx \frac{U_{DC}}{4\xi\omega_f L} H_{6\xi}\,, \tag{54a}$$

where:

$$H_{6\xi} = \sqrt{\sum_{n=1,3,5,7,9} \left(\hat{F}^{(*)}_{6\xi+n}\right)^2}\,. \tag{54b}$$

Table 2 contains the value of the $H_{6\xi}$ coefficients.

Table 2
The value of the $H_{6\xi}$ coefficients

M	0.0	0.05	0.1	0.2	0.3	0.4
$H_{6\xi}$	0.000	0.049	0.089	0.126	0.104	0.091
M	0.5	0.6	0.7	0.8	0.9	1. 0
$H_{6\xi}$	0.115	0.112	0.094	0.108	0.115	0.097

6.2. The LCRL filter capacitor current harmonics forced by the distorted AC current of AFE converters. Using the superposition method, we can determine the *rms* values of capacitor current harmonics C forced by the distorted AC current of AFE converters taking into account only the second component of the right-hand side of Eq. (41).

$$\underline{I}_{c(AFE),k} = -\frac{Z_{ab,k}C}{L'_\sigma\left(1+j\omega_k R_t C\right)}\left(\underline{U}'_{afe1,k}+\underline{U}'_{afe2,k}\right). \tag{55}$$

According to the considerations in Chapter 5, the sum of the voltages of u_{afe1} and u_{afe2} contains harmonics of the order of $k = \rho\xi_{afe} + n$ for $n = \pm1, \pm3, \pm5\ldots$ and for $\rho = 0, \pm4, \pm8\ldots$

For $k = n$ assuming odd values and $\rho = 0$ current amplitude value $\hat{I}_{c(AFE),k}$ can be calculated from the formula:

$$\widehat{I}_{c(AFE),n} = \frac{4Z_{ab,n}C}{L'_\sigma\sqrt{1+\left(\omega_n R_t C\right)^2}}\frac{U'_{dc,afe}}{2}\hat{F}_n^{(afe)}, \tag{56}$$

where $\hat{F}_{0n}^{(afe)} = \left|F_{0n}^{(afe)}\right|$, $F_{0n}^{(afe)} = F_{0n}(M_{afe})$ is described by (5) and $Z_{ab,n}$ is given by the formula (44) for $k = n$, $U'_{dc,afe}$ is the AFE DC-link voltage referenced to the "a–b" output of the power supply unit.

After substituting $n = 1$ into (56) and the relation (44) describing $Z_{ab,1}$ and making several transformations and applying approximation $\hat{F}_{01}^{(afe)} \approx M_{afe}$ we get:

$$\widehat{I}_{c(AFE),1} = \frac{C}{L'_\sigma}\frac{2\omega_f L_z}{\sqrt{\left(\omega_f C R_t\right)^2+\left(1-\omega_f^2/\omega_{res}^2\right)^2}}U'_{dc,afe}M_{afe}. \tag{57}$$

Because $10\omega_f < \omega_{res}$ [14] and $\left(\omega_f C R_t\right)^2 \ll 1$, relation (57) can be simplified to form:

$$\widehat{I}_{c(AFE),1} = 2\left(L_z/L'_\sigma\right)\omega_f C U'_{dc,afe}M_{afe}. \tag{58}$$

For n taking odd values and ρ taking values of $\pm4, \pm8\ldots$, values of capacitor current harmonics of the order $k = \rho\xi_{afe} + n$ can be determined from the relation:

$$\widehat{I}_{c(AFE),\rho n} = 2\frac{Z_{ab,k}CU'_{dc,afe}\hat{F}_{\rho n}^{(afe)}}{L'_\sigma\sqrt{1+\left(\omega_k R_t C\right)^2}}, \tag{59}$$

where $\hat{F}_{\rho n}^{(afe)} = \left|F_{\rho n}^{(afe)}\right|$, $F_{\rho n}^{(afe)}$ are described by (10).

Figure 10e shows the spectrum of harmonic current of capacitor C. The dominant harmonics of the higher order are harmonics of $4\xi_{afe} + n$ orders (for $n = -5, -3, -1, 1, 3, 5$) and except for the basic harmonic these harmonics have a decisive influence on the *rms* value of capacitor current . The resultant *rms* value of harmonic of $4\xi_{afe} - 5 \div 4\xi_{afe} + 5$ orders of the capacitor current can be determined from the following relation:

$$I_{c(AFE),4\xi afe} \approx 2\frac{Z_{ab,4\xi afe}CU'_{dc,afe}H_{4\xi afe}}{L'_\sigma\sqrt{1+\left(\omega_{4\xi afe}R_t C\right)^2}}, \tag{60a}$$

where:

$$H_{4\xi afe} = \sqrt{\sum_{n=1,3,5}\left(\hat{F}_{4\xi_{afe}+n}^{(afe*)}\right)^2}. \tag{60b}$$

$\hat{F}_{\rho\xi afe+n}^{(afe*)}$ is described by (53) for M_{afe} modulation depth factor. After substituting $Z_{ab,4\xi afe}$ in (60) described by (44) and making several transformations and then taking into account the inequality $\omega_{4\xi afe}CR_t \ll \omega_{4\xi_{afe}}^2/\omega_{res}^2$, (59) may be presented in the form of:

$$I_{c(AFE),4\xi afe} \approx \frac{2\omega_{4\xi afe}U'_{dc,afe}}{\left(\omega_{4\xi afe}^2-\omega_{res}^2\right)L'_\sigma}H_{4\xi afe}, \tag{61}$$

where $\omega_{4\xi afe} = 4\xi_{afe}\omega_f$.

Table 3 shows the value of $H_{4\xi afe}$ coefficient for M_{afe} parameter.

Table 3
Value of $H_{4\xi afe}$ coefficient

M_{afe}	0.55	0.6	0.65	0.7	0.75
$H_{4\xi afe}$	0.133	0.137	0.148	0.162	0.173
M_{afe}	0.8	0.85	0.9	0.95	1.0
$H_{4\xi afe}$	0.177	0.174	0.165	0.151	0.137

7. RMS value of the basic harmonic current of the capacitor C

Neglecting the voltage drops across the L and L'_σ inductances coming from the harmonics of the basic currents flowing through these inductances, one can assume the following equality

$$U_{DC}M = U'_{dc,afe}M_{afe} = \hat{U}_{ab,1}, \tag{62}$$

where $\hat{U}_{ab,1}$ is the fundamental harmonic of voltage between "a–b" terminals.

Furthermore, it can be assumed that the basic harmonics of the currents in a capacitor $\hat{I}_{c(INV),1}$ and $\hat{I}_{c(AFE),1}$ are in phase, so the components described in relation (48) and (58) can be added. The *rms* value $I_{c,1}$ of the fundamental harmonic current of the capacitor C is described by the equation:

$$I_{c,1} = 0.707\omega_f C\hat{U}_{ab,1}. \tag{63}$$

Formula (63) is obvious, but its derivation confirms the validity of dependencies (48) and (58) and the analysis carried out in Sections 6.1 and 6.2.

8. The transfer function of the LCRL-filter

The main harmonic current source of the LCRL filter capacitor is the AFE rectifier. Therefore, we are interested in the LCRL-filter transfer function defined as:

$$G_{is}(s) = \frac{-I_{s(AFE)}(s)}{U'_{afe1}(s) + U'_{afe2}(s)}, \tag{64}$$

where: $I_{s(AFE)}(s)$ is the Laplace's transform of the current component $i_s(t)$ forced by AFE converters.

The minus sign results from the accepted direction of the current i_s in Fig. 7. The complex value of the harmonics of the current component $i_s(t)$ forced by AFE converters is described by the relation:

$$\underline{I}_{s(AFE),k} = -\frac{2}{3}\frac{\underline{U}_{ab(AFE),k}}{j\omega_k L}. \tag{65}$$

The second component of equation (39) is the voltage component at terminals ab forced by the AC voltages of AFE converters.

$$\underline{U}_{ab(AFE),k} = \frac{\underline{Z}_{ab,k}}{j\omega_k L'_\sigma}\left(\underline{U}'_{afe1,k} + \underline{U}'_{afe2,k}\right). \tag{66}$$

From relations (65) and (66) the following can be determined:

$$\frac{-\underline{I}_{s(AFE),k}}{\underline{U}'_{afe1,k} + \underline{U}'_{afe2,k}} = -\frac{2}{3}\frac{\underline{Z}_{ab,k}}{\omega_k^2 L L'_\sigma}. \tag{67}$$

After substituting relation (38) into (67) and making a few transformations we get:

$$\frac{-\underline{I}_{s(AFE),k}}{\underline{U}'_{afe1,k} + \underline{U}'_{afe2,k}} = -\frac{3j}{\omega_k} \cdot \frac{1 + j\omega_k C R_t}{j\omega_k C R_t\left(4L + 3L'_\sigma\right) + 4L + 3L'_\sigma - 2\omega_k^2 C L L'_\sigma}. \tag{68}$$

The transmittance module $\mathrm{G}_{is}(\mathrm{j}\omega)$ can be presented replacing $j\omega_k$ by $j\omega$ depending on (68):

$$|G_{is}(j\omega)| = \frac{3}{\omega} \cdot \sqrt{\frac{1 + (\omega C R_t)^2}{\left(4L + 3L'_\sigma - 2\omega^2 C L L'_\sigma\right)^2 + (\omega C R_t)^2\left(4L + 3L'_\sigma\right)^2}}. \tag{69}$$

Figure 8 shows a Bode diagram of the LCRL filter with the selected parameters. The value of the damping resistance R_t was selected based on the criterion given in [2, 16] $R_t = 1/(6\omega_{res}C)$. The absolute value $|G_{is}(j\omega)|$ is maximum for $f \approx 790$ Hz. The reduction of this value can be achieved by increasing the value of capacitance C and/or inductance L. The value of inductance L is limited by its dimensions and the required value of the minimum slope of the output current of each branch of the inverter. Increasing the C value, on the other hand, increases the reactive power taken from the power supply. Using several AFE sections with synchronized auxiliary carrier wave [8] increases the minimum value of the harmonic order of the current drawn from the power supply output.

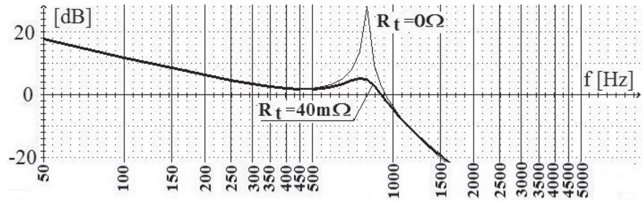

Fig. 8. Bode diagram of the LCRL filter with the chosen parameters: $L = 200$ μH, $L'_\sigma = 150$ μH, $R_t = 0$ Ω, $R_t = 40$ mΩ, $C = 840$ μF

9. Selection of capacitor capacity in DC circuit

If we omit the voltage drop across inductance L for the fundamental component, we can write:

$$I_{cDC,rms} = 0.707P/U_{DC}, \tag{70}$$

where P is the active power taken from "a–b" output.

The voltage ripple amplitude on the inverter capacitor C_{DC} can be determined from the relation:

$$U_{cDC,p} = 0.707 I_{cDC,rms}/\left(\omega_f C_{DC}\right). \tag{71}$$

For $P = 1200$ kW, $U_{DC} = 630$ V, $f_f = 16.67$ Hz, $C_{DC} = 153$ mF we get $I_{cDC,rms} = 1390$ A. This means that in a state of overload of the power supply ($P = 2P_{nom}$) for the system 16.67 Hz the ripple rate defined as $U_{cDC,p}/U_{DC} \cdot 100\%$ will not exceed 10%.

10. Simulation studies

Simulation data was performed in the Turbo Pascal package. The simulation tests, the results of which are shown in Figs. 9 and 10, were performed for the sinusoidal signal that sets the output voltage. Simulation tests were carried out for the system shown in Fig. 1. The equivalent diagram of the tested system is shown in Fig. 7. The transformer $T_{r,afe}$ is represented by the leakage inductance L'_σ while the leakage inductance of the transformer T_{r2} of much smaller value than L'_σ was omitted in the numerical model.

The parameters of the numerical model have values: $M = 0.9$, $U_{DC}^{(base)} = 2$ V, $C_{DC} = 153$ mF, $L = 200$ μH, $C = 840$ μF, $R_t = 40$ mΩ, $U'^{(base)}_{dc,afe} = 2.4$ V, AFE dc-link capacitance $C'_{afe} = 324$ mF, $M_{afe} = 0.75$, $L'_\sigma = L'_{\sigma 25} = 150$ μH, AFE dc-load $R'_{dc,afe} = 0.95$ Ω, $f_f = 50$ Hz, $f_c = 2$ kHz, $f_c^{(afe)} = 500$ Hz.

The time courses of currents i_1, i_2, i_3, i_s, i'_{afe1}, i'_{afe2}, i'_{afe} and u_{ab} voltage for U_{DC} voltage of the value which is in the real

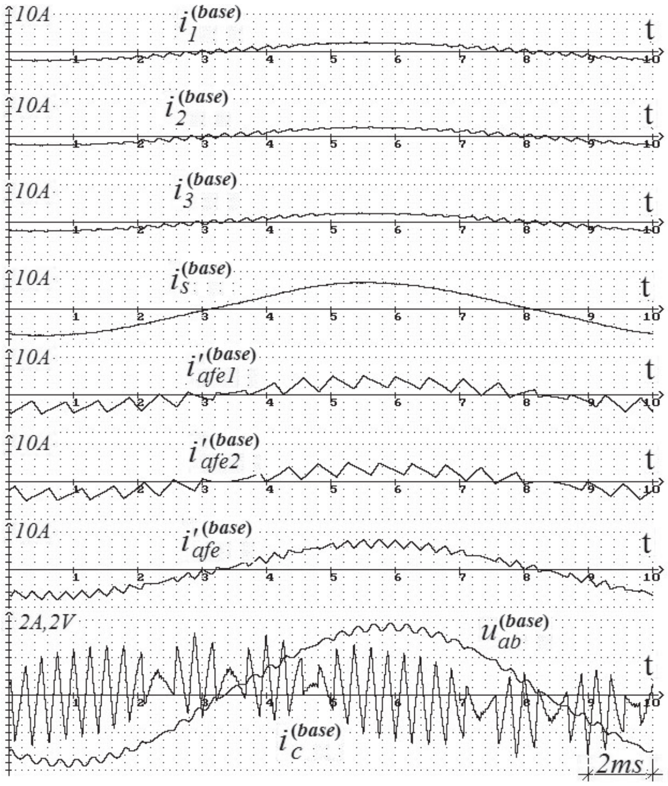

Fig. 9. Simulation of i_1, i_2, i_3 currents, their sum i_s and i'_{afe1}, i'_{afe2}, i_{afe}, i_c currents and u_{ab} voltage in the system shown in Fig. 1.

system ($U_{DC} = 630$ V, $U_{dc,afe} = 3400$ V) have the same shape as the courses shown in Fig. 9 and the following relationships are met:

$$i_x = i_x^{(base)} \left(U_{DC}/U_{DC}^{(base)} \right), \tag{72}$$

$$i'_x = i'^{(base)}_x \left(U_{DC}/U_{DC}^{(base)} \right), \tag{73}$$

where $i'_x = \upsilon_{41} i_x$, υ_{41} is the product of coil ratios of transformers T_{r2} and $T_{r,afe}$ ($\upsilon_{41} = z4/z1 = 4.5$).

Ratio value υ_{41} is usually fixed for both power supply and traction vehicle systems (25 kV and 15 kV) but $L'_{\sigma 15}$ is greater than $L'_{\sigma 25}$.

The equations for u_{ab} and $U_{DC,afe}$ are as follows:

$$u_{ab} = u_{ab}^{(base)} \left(U_{DC}/U_{DC}^{(base)} \right), \tag{74}$$

$$U'_{DC,afe} = U'^{(base)}_{dc,afe} \left(U_{DC}/U_{DC}^{(base)} \right), \tag{75}$$

$$U_{DC,afe} = \upsilon_{41} U'_{DC,afe}. \tag{76}$$

On the basis of the results in Table 4 it is possible to calculate the resultant *rms* value of current harmonics $I_{afe1,k}$ for $k = 15 \div 25$ according to below formula:

$$I_{afe1,2\xi afe} = \frac{1}{\upsilon_{41}} \frac{\sqrt{2}}{2} \frac{U_{DC}}{U_{DC}^{(base)}} \sqrt{\sum_{k=15,17,\ldots,25} \left(\hat{I}'^{(base)}_{afe1,k} \right)^2}. \tag{77}$$

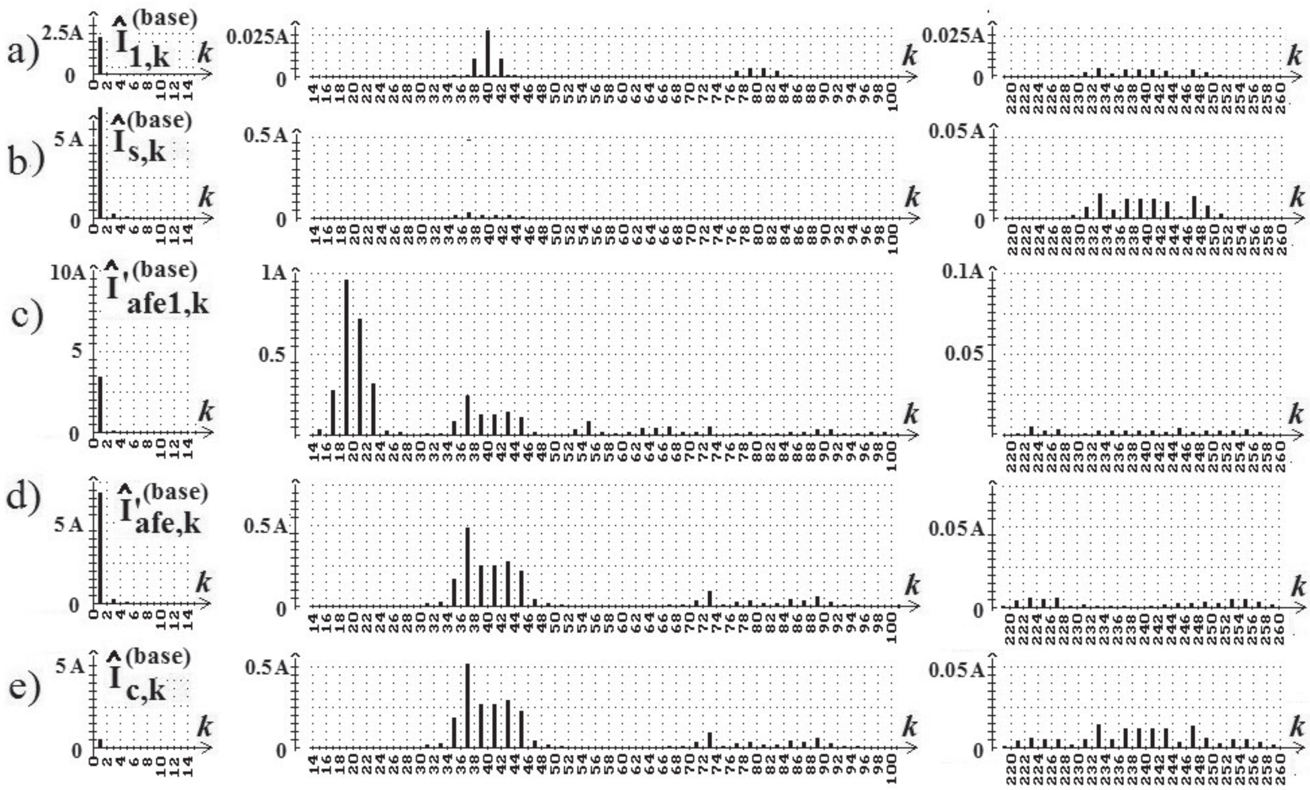

Fig. 10. a) i_1, b) i_s, c) i'_{afe1}, d) i_{afe} and e) i_c harmonic current spectra with time courses shown in Fig. 9

After substituting the data to (77) we get $I_{afe1,2\xi afe} = 62.84\ A_{rms}$.

On the basis of the results gathered in Table 4 it is possible to calculate the resultant *rms* value of current harmonics $I_{c,k}$ for $k = 35 \div 45$ according to below formula:

$$I_{c.4\xi afe} = \frac{\sqrt{2}}{2} \frac{U_{DC}}{U_{DC}^{(base)}} \sqrt{\sum_{k=35,37\ldots45} \left(\hat{I}_{c,k}^{(base)}\right)^2}. \tag{78}$$

After substituting the data, we get $I_{c,4\xi afe} = 169\ A_{rms}$ while substituting the parameters of the simulation model to formula (61), we obtain $I_{c,4\xi afe} = 164\ A_{rms}$.

Table 4
Results of simulations research

k	15	17	19	21	23	25
$\hat{I}'^{(base)}_{afe1,k}$	0.030	0.275	0.962	0.713	0.318	0.025
k	35	37	39	41	43	45
$\hat{I}^{(base)}_{c,k}$	0.180	0.518	0.263	0.268	0.293	0.225
k	231	233	235	237	239	241
$\hat{I}^{(base)}_{c,k}$	0.005	0.014	0.005	0.012	0.011	0.012
k	243	245	247	249		
$\hat{I}^{(base)}_{c,k}$	0.012	0.003	0.013	0.005		

On the basis of the results gathered in Table 4 it is possible to calculate the resultant *rms* value of current harmonics $I_{c,6k}$ for $k = 231 \div 249$ according to below formula:

$$I_{c.6\xi} = \frac{\sqrt{2}}{2} \frac{U_{DC}}{U_{DC}^{(base)}} \sqrt{\sum_{k=231,233,\ldots,249} \left(\hat{I}_{c,k}^{(base)}\right)^2}. \tag{79}$$

After substituting the data to (79) we get $I_{c,6\xi} = 7.1\ A_{rms}$ while substituting the parameters of the simulation model to formula (54a), we get $I_{c,6\xi} = 7.2\ A_{rms}$.

Figure 11 shows the $u_{ab}^{(base)}$ and $i_c^{(base)}$ waveforms obtained for numerical model without load ($i_{afe} = 0$). The following results were also obtained: fundamental harmonic amplitude $\hat{I}_{c,1}^{(base)} = 0.158$ A and *rms* value $I_c^{(base)} = 0.115\ A_{rms}$. Based on the obtained results it is possible to determine the amplitude $\hat{I}_{c,1} = 49.8$ A and the *rms* value $I_c = 36.2\ A_{rms}$ of C capacitor current and then the rms value of the component containing higher harmonics $I_{c,h} = 8.4\ A_{rms}$.

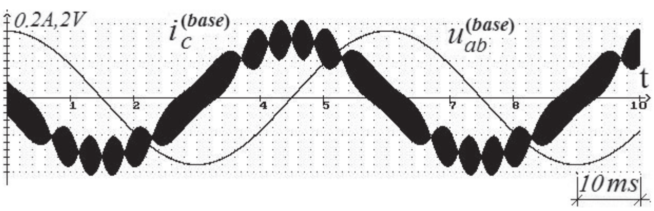

Fig. 11. Simulation of i_c current and u_{ab} voltage in the system shown in Fig. 1 without load ($i_{afe} = 0$)

11. Experimental testing of the power supply

Operational tests were carried out in MEDCOM company, on the test bench equipped with power supply system, measuring equipment and load set of high-power resistors (100 kW) and a battery of capacitors with reactive power of 120 kVAr. Examples of measurement results are shown in the oscillograms (Figs. 12–16).

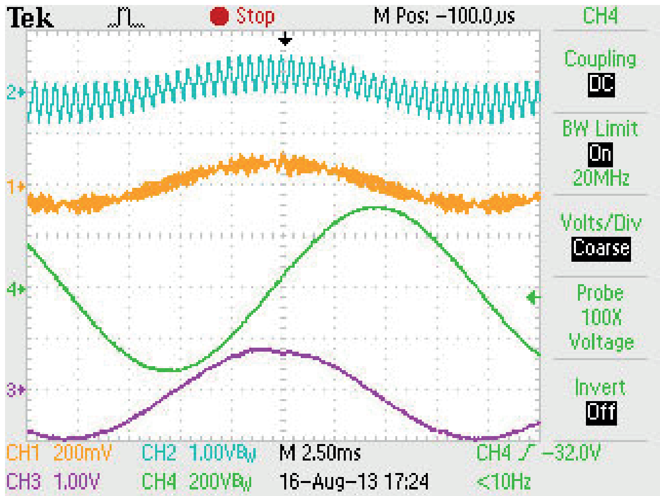

Fig. 12. Oscillograms of the output currents of two branches in an experimental half-bridge system with carrier signals u_{T1}, $u_{T1\_}$ for $f_c = 2$ kHz for resistive-capacitive load of the power supply unit CH1: i_c (200 A/div.), CH2: i_1 (1000 A/div.), CH3: i_s (1000 A/div.), CH4: u_c (200 V/div.) for $L = 100$ µH and $C = 840$ µF

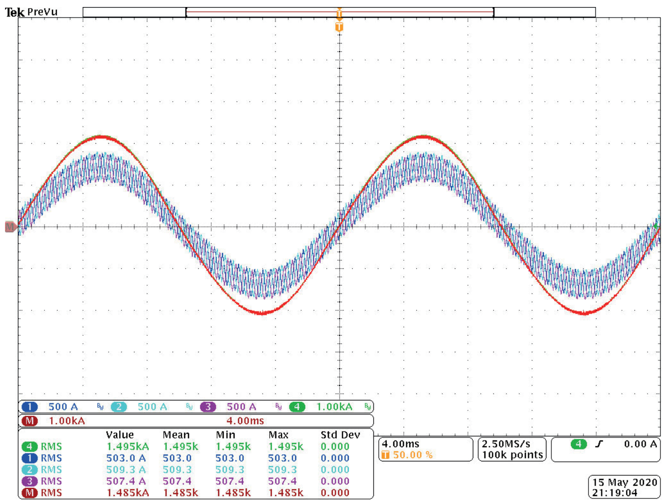

Fig. 13. Oscillograms of the output currents of three branches and the sums of these currents in the system for a short circuit state at the output: CH1: i_1 (500 A/div.), CH2: i_2 (500 A/div.), CH3: i_3 (500 A/div.), CH4: i_s(1000 V/div.) for $L = 200$ µH

11.1. Idle and short circuit power supply test. The tests were carried out without load and in short-circuit states for the system with current coupling, allowing to shape the sinusoidal current of a given value.

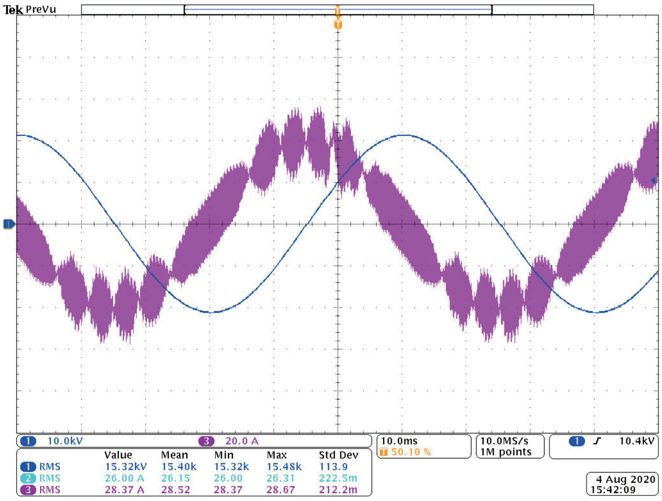

Fig. 14. Oscillogram of the HV output voltage for 15 kV/16$\frac{2}{3}$ Hz without load (CH1: 10 kV/div.) and oscillogram of the C capacitor current i_c (CH3: 20 A/div.) for $L = 200$ μH and $C = 840$ μF

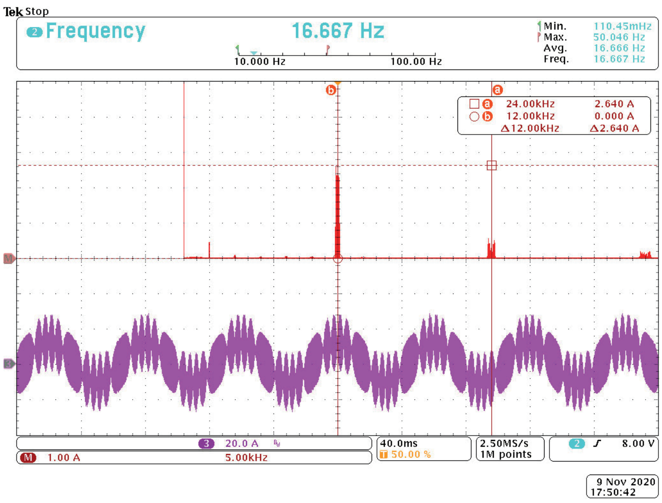

Fig. 15. Harmonics spectrum of the C capacitor current i_c for 16$\frac{2}{3}$ Hz system without load (M: 1 A/div.) and oscillogram of the C capacitor current i_c (CH3: 20 A/div.) for $L = 200$ μH and $C = 200$ μF

The i_c current shown in Fig. 14 (CH3) contains a fundamental component whose *rms* value can be calculated on the basis of (63) and a component containing sideband harmonics of the order $6\xi \pm n$. Signal shapes shown in Figs. 11 and 14 are characterized by very high similarity. Figure 15 shows the spectrum of the harmonics of the current i_c in a 15 kV/16. 67 Hz system without load for $L = 200$ μH and $C = 200$ μF. The frequencies of the dominant higher harmonics of the i_c current assume values close to 12 kHz.

11.2. AFE test in traction drive. Figure 16 shows oscillograms of traction voltage, currents drawn by two of the AFE rectifiers and DC-link voltage in the train locomotive (one head).

The $T_{r,afe}$ transformer dispersion inductances $L_{\sigma 25}$ related to the low-voltage side of the power supply unit can be determined

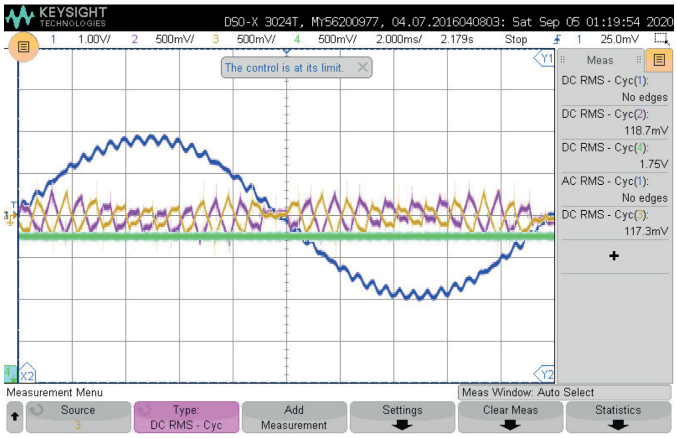

Fig. 16. Waveforms of traction voltage (CH1, 20 kV/div.), input AFE1 (CH2) and AFE2 (CH3) current (266.6 A/div) and the u_{dc_afe} (CH4, 1 kV/div.) without load for $L_{\sigma 25} = 3.25$ mF and $\upsilon_{41} = 4.5$

from the formula $L'_\sigma = L_{\sigma 25}/\upsilon_{42}^2$ and their values are 160 μH. On the basis of the obtained values shown in the right part of the waveform the *rms* values of I_{afe1} and I_{afe2} currents can be calculated. The gain of the measuring system is 1600 A/3 V. The *rms* value of $I_{afe1} = 0.1187 \cdot 1600/3$ ($I_{afe1} = 63.3$ A_{rms}) and $I_{afe2} = 0.1173 \cdot 1600/3$ ($I_{afe2} = 62.6$ A_{rms}). The *rms* value of I_{afe1} current obtained from formula (77) on the basis of data and simulation results was 62.8 A_{rms}.

12. Conclusions

A control system with three modulator carrier signals ensures that the *rms* value of the LCRL output filter capacitor current of the inverters is minimized to such an extent that the main source of the LCRL filter capacitor current harmonics is the AFE rectifier load. The analysis of these harmonics allows the selection of LCRL filter capacitor parameters. The serial structure of one voltage controller and current controllers in the amount equal to the number of transistor branches allows for parallel connection of power supplies.

Related to the results obtained in the real system, the relative error of the simulation test results is no more than 5%. The relative error of the verified simulation test results obtained on the basis of the derived dependencies for the rated operating conditions of the power supply does not exceed 15%.

References

[1] L. Asiminoaei, E. Aeloiza, P.N. Enjeti, and F. Blaabjerg, "Shunt Active-Power-Filter Topology Based on Parallel Interleaved Inverters", *IEEE Trans. Ind. Electron.* 55(3), 1175–1189 (2008), doi: 10.1109/TIE.2007.907671.

[2] H.-G. Jeong, D.-K. Yoon, and K.-B. Lee, "Design of an LCL-Filter for Three-Parallel Operation of Power Converters in Wind Turbines", *J. Power Electron.* 13(3), 437–446 (2013), doi: 10.6113/JPE.2013.13.3.437.

[3] T. Platek, "Analysis of Ripple Current in the Capacitors of Active Power Filters", *Energies* 12(23), 1–31 (2019), doi: 10.3390/en12234493.

[4] D. Shin, H.-J. Kim, J.-P. Lee, T.-J. Kim, and D.-W. Yoo, "Coupling L-CL Filters and Active Damping Method for Interleaved Three-Phase Voltage Source Inverters", in *2015 17th European Conference on Power Electronics and Applications (EPE'15 ECCE-Europe)*, Geneva, 2015, pp. 1–10, doi: 10.1109/EPE.2015.7309318.

[5] G.G. Balazs, M. Horvath, I. Schmidt, and P. Kiss, "Examination of new current control methods for modern PWM controlled AC electric locomotives", in *6th IET International Conference on Power Electronics, Machines and Drives (PEMD 2012)*, Bristol, 2012, pp. 1–5, doi: 10.1049/cp.2012.0314.

[6] P. Falkowski, A. Sikorski, K. Kulikowski, and M. Korzeniewski, "Properties of active rectiefier with LCL filter in the selection process of the weighting factors in finite control set-MPC", *Bull. Pol. Acad. Sci. Tech. Sci.* 68(1), 51–60 (2020), doi: 10.24425/bpasts.2020.131836.

[7] J. Michalik, J. Molnar, and Z. Peroutka, "Optimal Control of Traction Single-Phase Current –Source Active Rectifier", in *Proceedings of 14th International Power Electronics and Motion Control Conference EPE-PEMC 2010*, Ohrid, 2010, pp. T9-82-T9-88, doi: 10.1109/EPEPEMC.2010.5606604.

[8] L.Di. Donna, F. Liccardo, P. Marino, C. Schiano, and M. Triggianese, "Single-phase synchronous active front-end for high power applications," in *Proceedings of the IEEE International Symposium on Industrial Electronics, 2005. ISIE 2005*, Dubrovnik, Croatia, 2005, vol. 2, pp. 615–620, doi: 10.1109/ISIE.2005.1528987.

[9] D.G. Holmes, T.A. Lipo, *Pulse Width Modulation For Power Converters*, pp. 125–146, IEEE PRESS, Willey-Interscience. Copyright, 2003.

[10] W. Wu, M. Huang, and F. Blaabjerg, "Efficiency comparison between the LLCL and LCL-filters based single-phase grid-tied inverters", *Arch. Electr. Eng.* 63(1), 63–79 (2014), doi: 10.2478/aee-2014-0005.

[11] M. Liserre, F. Blaabjerg, and S. Hansen, "Design and Control of an LCL-Filter-Based Three-Phase Active Rectifier", *IEEE Trans. Ind. Appl.* 41(5), 1281–1291 (2005), doi: 10.1109/TIA.2005.853373.

[12] K. Jalili and S. Bernet, "Design of LCL Filters of Active-Front-End Two-Level Voltage-Source Converters", *IEEE Trans. Ind. Electron.* 56(5), 1674–1689, (2009), doi: 10.1109/TIE.2008.2011251.

[13] S. Piasecki, R. Szmurlo, J. Rabkowski, and M. Jasinski, "Dedicated system for design, analysis and optimization of AC-DC converters", *Bull. Pol. Acad. Sci. Tech. Sci.* 64(4), 897–905 (2016).

[14] F. Liu, X. Zha, Y. Zhou, and S. Duan, "Design and research on parameter of LCL filter in three-phase grid-connected inverter", in *Power Electronics and Motion Control Conference, 2009. IPEMC '09. IEEE 6th International*, May 2009, pp. 2174 –2177, doi: 10.1109/IPEMC.2009.5157762.

[15] M.A. Abusara, M. Jamil, and S. M. Sharkh, "Repetitive current control of an interleaved grid connected inverter", in *Proc. 3rd IEEE Int. Symp. Power Electron. Distrib. Gener. Syst. (PEDG)*, Aalborg, 2012, pp. 558–563, doi: 10.1109/PEDG.2012.6254057.

[16] A.A. Rockhill, M. Liserre, R. Teodorescu, and P. Rodriguez, "Grid-Filter Design for a Multimegawatt Medium-Voltage Voltage-Source Inverter", *IEEE Trans. Ind. Electron.* 58(4), 1205–1217 (2011), doi: 10.1109/TIE.2010.2087293.